Chin. Geogra. Sci. 2022 Vol. 32 No. 2 pp. 285−301
https://doi.org/10.1007/s11769-022-1262-8

Springer Science Press
www.springerlink.com/content/1002-0063

Spatio-temporal Variations of Temperature and Precipitation During 1951–2019 in Arid and Semiarid Region, China

HUANG Yufei[1], LU Chunyan[1, 2, 3], LEI Yifan[1, 3, 4], SU Yue[1, 3], SU Yanlin[1, 4], WANG Zili[1, 4]

(1. *College of Computer and Information Sciences*, *Fujian Agriculture and Forestry University*, *Fuzhou* 350002, *China*; 2. *Key Laboratory of Ecology and Resources Statistics of Fujian Province Universities*, *Fujian Agriculture and Forestry University*, *Fuzhou* 350002, *China*; 3. *Statistical Information Research Center of Fujian Province*, *Fujian Agriculture and Forestry University*, *Fuzhou* 350002, *China*; 4. *Research Centre of Resource and Environment Spatial Information Statistics of Fujian Province*, *Fujian Agriculture and Forestry University*, *Fuzhou* 350002, *China*)

Abstract: Understanding the spatio-temporal variations of temperature and precipitation in the arid and semiarid region of China (ASRC) is of great significance for promoting regional eco-environmental protection and policy-making. In this study, the annual and seasonal spatio-temporal patterns of change in average temperature and precipitation and their influencing factors in the ASRC were analyzed using the Mann-Kendall test, linear tendency estimation, accumulative anomaly and the Pearson's correlation coefficient. The results showed that both annual average temperature and average annual precipitation increased in the ASRC during 1951–2019. The temperature rose by about 1.93℃ and precipitation increased by about 24 mm. The seasonal average temperature presented a significant increase trend, and the seasonal precipitation was conspicuous ascension in spring and winter. The spatio-temporal patterns of change in temperature and precipitation differed, with the southwest area showing the most obvious variation in each season. Abrupt changes in annual and seasonal average temperature and precipitation occurred mainly around the 1990s and after 2000, respectively. Atmospheric circulation had an important effect on the trends and abrupt changes in temperature and precipitation. The East Asian summer monsoon had the largest impact on the trend of average annual temperature, as well as on the abrupt changes of annual average temperature and precipitation. Temperature and precipitation changes in the ASRC were influenced by long-term and short-term as well as direct and indirect anthropogenic and natural factors. This study identifies the characteristics of spatio-temporal variations in temperature and precipitation in the ASRC and provides a scientific reference for the formulation of climate change responses.

Keywords: multi-source remote sensing data; temperature; precipitation; arid and semiarid region; spatio-temporal variation; atmospheric circulation

Citation: HUANG Yufei, LU Chunyan, LEI Yifan, SU Yue, SU Yanlin, WANG Zili, 2022. Spatio-temporal Variations of Temperature and Precipitation During 1951–2019 in Arid and Semiarid Region, China. *Chinese Geographical Science*, 32(2): 285−301. https://doi.org/10.1007/s11769-022-1262-8

1 Introduction

Climate change is one of the most important issues that countries are facing across the world. Global warming has become increasingly prominent since the 1980s (Kerr, 2007). Although a series of inter-governmental cooperation frameworks and conventions have been implemented, e.g., the United Nations Framework Convention on Climate Change and Kyoto Protocol, extreme weather events caused by climate change, such as

Received date: 2021-07-27; accepted date: 2021-10-25
Foundation item: Under the auspices of Fujian Natural Science Foundation General Program (No. 2020J01572), the Scientific Research Project on Outstanding Young of the Fujian Agriculture and Forestry University (No. XJQ201920)
Corresponding author: LU Chunyan. E-mail: luchunyan@fafu.edu.cn

droughts, floods, hurricanes and rainstorms occurred frequently (Press, 2008). Hurricane 'Katrina' in 2005 and cyclone 'Nargis' in 2008 paralyzed cities and killed tens of thousands of people in America and Myanmar, respectively (McGregor, 2010; Raker et al., 2019). Bushfires in Australia lasted for nearly four months at the end of 2019 causing substantial economic and ecological losses (Schweinsberg et al., 2020). China is also prone to extreme weather events, with devastating floods in the Nenjiang and Songhua rivers in Northeast China in 1998 and droughts with varying degrees of severity in different regions of China since 2000 (Song, 2015). The economic losses caused by extreme weather events are substantial. For example, the direct damages arising from super typhoons 'Rainbow' in 2015 and 'Meranti' in 2016 both have cost more than 20 billion yuan (RMB) (Li, 2019; Zhao, 2019). Consequently, large-scale studies of climate change and its driving mechanisms are necessary to initialize models or set benchmarks. Temperature and precipitation, as the pivotal climate factors, have an extensive and far-reaching impact on human well-being, vegetation growth and wildlife survival, among other aspects. Therefore, it is of great significance to understand the variation characteristics of temperature and precipitation for socio-economic and ecological sustainability.

Numerous studies have been conducted on the spatio-temporal trends and abrupt changes of temperature and precipitation. Many studies have focused on analyzing annual and seasonal variations in individual meteorological factors using annual and monthly observations from meteorological stations, based on linear tendency estimation, empirical orthogonal function and sliding *t* test methods. These studies found that in recent years, different regions showed different degrees of warming (Peterson and Vose, 1997; Hansen et al., 2001; Mao et al., 2018a; Song and Park, 2020; Li et al., 2021b), while the trends and characteristics of precipitation varied from region to region, making them difficult to understand (Dai et al., 1997; Shi et al, 2019; Carrasco and Cordero, 2020; Li et al., 2020a; Yan et al., 2021).

Recent developments on temperature and precipitation studies have improved the accuracy in different temporal dimensions such as daily, ten-daily, monthly and yearly. Research methods not only have diversified, but also the combined analysis of time and space dimensions has widely applied. Studies also tend to combine multiple climatic factors. Since 1951, the trends in temperature and precipitation in China have changed significantly. Based on linear tendency estimation and Mann-Kendall (M-K) test, Ge et al. (2011) and Wang et al. (2013) analyzed the spatio-temporal variations of annual and monthly temperature and precipitation in China, respectively. Their results showed that the temperature rise was more obvious in the past 50 yr in China, and the regional precipitation differences were significant since 1970 with floods in the south and droughts in the north. Based on the anomaly analysis and wavelet analysis, Zhao and Luo (2021) used annual average temperature and precipitation observation data to analyze their periodicity on multiple time scales in west Anhui. The results indicated that the temperature rose steadily from 1960 to 2013 while precipitation showed five alternating periods of drying and wetting. Moreover, the temperature and precipitation changes in other places, such as the lower Yellow River region, the Songhua River Basin, the Huaihe River Basin, Yunnan Province, have also been explored using spatial interpolation, correlation coefficients and linear regression, *etc.* (Lu et al., 2014; Chen, 2015; Gou et al., 2020; Xu et al., 2021).

As one of the most fragile ecosystems, the arid and semiarid region of China (ASRC) has received attentions on its temperature and precipitation changes. Although changes in climate factors related to atmospheric circulation have been verified in different arid and semiarid regions on Earth (Li et al., 2014; Feng et al., 2016; Wang et al., 2019; Zhang et al., 2020), there are few studies on the use of multiple atmospheric circulation models for analysis of the spatio-temporal variations of climate factors in these regions. In addition, most previous studies are not only limited to an individual meteorological factor and a single method for testing change, but also often lack validation. Thus, there is an urgent need to explore the characteristics of change in temperature and precipitation and the relationship with atmospheric circulation in arid and semiarid regions.

The arid and semiarid region of China is the largest arid zone in the middle latitudes of the Northern Hemisphere and is an important farming-pastoral transitional zone in China (Huang et al., 2019). In recent decades, the ASRC has expanded southeast owing to global warming, and the climate has changed markedly, which has had a profound influence on human and natural sys-

tems (Lyu et al., 2009; Ni, 2011). At present, research has focused on land cover change and vegetation degradation in the ASRC, but the relationship between the ASRC's climate and atmospheric circulation is rarely investigated. Given the importance of the eco-environment in the ASRC and the limitations of previous studies, the objectives of this research were to: 1) analyze the spatio-temporal trends and changes in temperature and precipitation; 2) explore the influence of atmospheric circulation on temperature and precipitation; and 3) identify the drivers affecting variations in temperature and precipitation. The study will provide references to sustainable socio-economic development, eco-environmental protection, and climate change response.

2 Materials and Methods

2.1 Study area

According to the classification standard of the Natural Zoning Commission of Chinese Academy of Sciences (Mao et al., 2018b), the study area, ASRC, was delineated using a drought index (the ratio of annual precipitation to annual potential evaporation) of less than 0.5 (Fig. 1). The study area is located in Northwest China, ranging from 73°29′E to 125°51′E and from 27°14′N to 50°08′N, covering an area of 4.56×10^6 km^2 and accounting for 47% of China's territory. It spans 12 provinces/autonomous regions from west to east, including Xinjiang, Tibet, Qinghai, Gansu, Inner Mongolia, Ningxia, Shaanxi, Shanxi, Hebei, Liaoning, Jilin and Heilongjiang. The landforms in this region are complex and diverse, mainly consisting of the Inner Mongolia Plateau, Loess Plateau, Qinghai-Tibet Plateau, Tarim Basin, Junggar Basin and Qaidam Basin. Most of the region has a temperate continental climate or a plateau alpine climate. Annual precipitation is less than 400 mm, decreasing from east to west (Wen et al., 2017).

2.2 Data sources and pre-processing

In this study, the monthly average temperature and monthly precipitation observations from 300 meteorological stations in and around the ASRC from 1951 to 2019 (Fig. 1) were collected as the basic data sources to analyze the trends, changes and spatial patterns of temperature and precipitation. The data were downloaded from the National Meteorological Information Center (http://data.cma.cn/). The quality of the meteorological data was strictly controlled. Missing or abnormal data accounted for less than 1% of the total data and were processed by referencing the method of Zhang et al. (2011). Monthly data were averaged to obtain seasonal and annual average data. Due to the wide application of the Spline interpolation in creating the continuous surfaces of meteorological factors (Jobst et al., 2017; Jia and Cui, 2018; Xu et al., 2018), the method was used to identify the spatial patterns of seasonal and annual average temperature and precipitation in the study. It should be noted that the seasons were divided into spring from March to May, summer from June to August, autumn from September to November and winter from Decem-

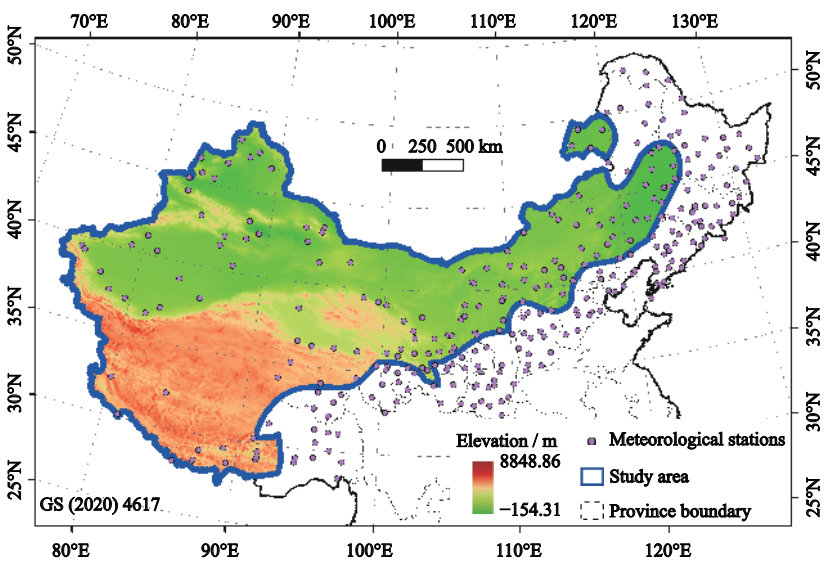

Fig. 1 Location of study area and meteorological stations

ber to February of the following year (Wen et al., 2017). Data on the population and total energy consumption were gathered from the China Economic and Social Big Data Research platform (http://data.cnki.net/) to explore their trends and correlation with climate factors.

Several large-scale oceanic atmospheric circulation indices, including the El Niño Southern Oscillation (ENSO) (downloaded from http://www.cpc.ncep.noaa.gov/), Arctic Oscillation (AO) (http://www.cpc.ncep.noaa.gov/), North Atlantic Oscillation (NAO) (http://ljp.gcess.cn/dct/page/1), Pacific Decadal Oscillation (PDO) (http://www.esrl.noaa.gov/psd/data/correlation/pdo.data), and the East Asian summer monsoon index (EASM) (http://ljp.gcess.cn/dct/page/1), were selected for correlation analysis with temperature and precipitation in the study.

2.3 Mann-Kendall test

To analyze the trends and abrupt changes of temperature and precipitation, the M-K test was selected to quantify the change degree and significance (Li et al., 2021a). The M-K test included M-K trend test and M-K abrupt change test, which the former was used to reflect the change trends, and the latter to identify abrupt changes. Assuming the time series of a certain climate element is (X_1, X_2, ..., X_n), the basic principle of M-K trend test is expressed as follows (Gocic and Trajkovic, 2013):

$$S = \sum_{i=2}^{n}\sum_{j=1}^{i-1}\mathrm{sgn}(X_i - X_j) \tag{1}$$

$$\mathrm{sgn}\left(X_i - X_j\right) = \begin{cases} 1, X_i - X_j > 0 \\ 0, X_i - X_j = 0 \\ -1, X_i - X_j < 0 \end{cases} \tag{2}$$

$$Z = \begin{cases} (S-1)/\sqrt{\mathrm{Var}(S)}, S > 0 \\ 0, S = 0 \\ (S+1)/\sqrt{\mathrm{Var}(S)}, S < 0 \end{cases} \tag{3}$$

$$\beta = \mathrm{median}\left(\frac{X_j - X_i}{j-i}\right), \forall 1 \le i \le j \le n \tag{4}$$

$$\mathrm{Var}(S) = \frac{n(n-1)(2n+5)}{18} \tag{5}$$

where S obeys a normal distribution. Var(S) is the variance of S. X_i and X_j are the climatic values of years i and j. n is the sample size. β represents the slope. For a given confidence level α, if $|Z| \ge Z_{1-\alpha/2}$, the time series data exist obvious up or down trend. A positive value of Z indicates an increasing trend, while a negative value indicates a decreasing trend. For example, when $|Z| \ge 1.96$, it means that the 95% confidence level test is passed. A positive β value indicates an upward trend, whereas a downward trend.

The M-K abrupt change test is calculated as follows:

$$s_k = \sum_{i=1}^{k} r_i,\ k = 1,2,\ldots,n \tag{6}$$

$$r_i = \begin{cases} 1,\ X_i > X_j \\ 0,\ X_i X_j \end{cases},\ j = 1,2,\ldots,i \tag{7}$$

where s_k is the cumulative number of $X_i > X_j$, k is the cumulative number of samples, and r_i is the order column. On the assumption that the time series is random and independent, define the statistic:

$$UF_k = \frac{s_k - E(s_k)}{\sqrt{\mathrm{Var}(s_k)}}, k = 1,2,\ldots,n \tag{8}$$

$$E(s_k) = \frac{k(k-1)}{4}, k = 1,2,\ldots,n \tag{9}$$

$$\mathrm{Var}(s_k) = \frac{k(k-1)(2k+5)}{72}, k = 1,2,\ldots,n \tag{10}$$

where $UF_1 = 0$, $E(s_k)$ and Var(s_k) are the mean value and variance of the cumulative count s_k, respectively. UF_k is the standard normal distribution, which is in the order of time series x (x_1, x_2, …, x_n). Given the significance level α, look up the normal distribution table. If $|UF_k| > U_\alpha$, it indicates that there is an obvious trend change in the sequence. The above procedure is applied to the inverse columns of time series x (x_n, x_{n-1}, ..., x_1), so that $UB_k = -UF_k$ ($k = n, n-1, \ldots, 1$) and $UB_1 = 0$.

According to the calculated UF_k and UB_k, their curves are plotted. When the value of UF_k or UB_k is more than (less than) 0, it indicates an upward (downward) trend of the sequence. When they pass the threshold, it indicates a significant upward or downward trend. The range beyond the critical lines is the time zone of the abrupt change. If two curves intersect and the intersection point is within the critical line, the time corresponding to the intersection point is when the abrupt change begins.

2.4 Linear tendency estimation

To explore the trend rate of temperature and precipitation at each meteorological station, the linear regression equation of temperature or precipitation series $\{y_i\}$ and

its corresponding time series $\{t_i\}$ can be established as follows (Li et al., 2020b):

$$\hat{y}_i = a + bt_i, i = 1, 2, \ldots, n \tag{11}$$

where $\hat{y}_i$ is the estimated value of y_i, a is the regression constant, and b is the regression coefficient, namely the change trend. When b is positive (negative), it indicates that the temperature or precipitation shows an upward (downward) trend with time. The least square method can be used to obtain the estimated value of a and b, namely $\hat{a}$ and $\hat{b}$, as follows:

$$\hat{b} = \frac{\sum_{i=1}^{n}\left(t_i - \bar{t}\right)(y_i - \bar{y})}{\sum_{i=1}^{n}\left(t_i - \bar{t}\right)^2} \tag{12}$$

$$\hat{a} = \bar{y} - \hat{b}t_i \tag{13}$$

$$\bar{t} = \frac{1}{n}\sum_{i=1}^{n} t_i \tag{14}$$

$$\bar{y} = \frac{1}{n}\sum_{i=1}^{n} y_i \tag{15}$$

where $\bar{t}$ and $\bar{y}$ are the mean values of t and y, respectively; n is the sample size.

In order to understand the fitting effect of the unary linear regression equation with the actual observation data, the regression equation need to be statistically tested. This study used the F test to show whether the sequence was linearly significant or not.

Assuming that there is no linear trend in the sequence, i.e., H_0: $b = 0$, then the statistic is:

$$F = \frac{U}{Q/(n-2)} \sim F(1, n-2) \tag{16}$$

$$U = \sum_{i=1}^{n}(\hat{y}_i - \bar{y})^2 \tag{17}$$

$$Q = \sum_{i=1}^{n}(y_i - \hat{y}_i)^2 \tag{18}$$

where U is the regression sum of squares and Q is the residual sum of squares.

Given significance level α, look up the critical value table of F distribution with (1, n–2) degrees of freedom, and the critical value F_α(1, n–2) can be obtained. When $F > F_\alpha$(1, n–2), the null hypothesis is rejected, and the linear trend of the sequence is considered significant. Otherwise, the null hypothesis is accepted, and the linear trend is not significant.

2.5 Accumulative anomaly method

To verify the accuracy of M-K abrupt change test results, the accumulative anomaly method was utilized. The accumulative anomaly formula of temperature or precipitation series $\{y_i\}$ and corresponding time t is established as follows (Zhong and Li, 2014):

$$\hat{y} = \sum_{i=1}^{t}(y_i - \bar{y}),\ t = 1, 2, \ldots, n \tag{19}$$

$$\bar{y} = \frac{1}{n}\sum_{i=1}^{n} y_i \tag{20}$$

where $\hat{y}$ is the accumulative anomaly value of temperature or precipitation, $\bar{y}$ is the mean value of y, and n is the sample size.

Calculate the accumulative anomaly values of the temperature at n times, and draw the accumulative anomaly curve for analysis, so that the long-term trend of temperature and precipitation changes and the approximate time of abrupt changes could be determined.

2.6 Pearson's correlation analysis

To analyze the degree of correlation between temperature, precipitation and atmospheric circulation indices, Pearson's correlation coefficient was used, which is widely used in the field of natural science. Assuming that there are two variables (x_1, x_2, ..., x_n) and (y_1, y_2, ..., y_n) with a sample size of n, the calculation formula of correlation coefficient r is (Sensuse et al., 2015):

$$r = \frac{\sum_{i=1}^{n}(x_i - \bar{x})(y_i - \bar{y})}{\sqrt{\sum_{i=1}^{n}(x_i - \bar{x})^2}\sqrt{\sum_{i=1}^{n}(y_i - \bar{y})^2}} \tag{21}$$

$$\bar{x} = \frac{1}{n}\sum_{i=1}^{n} x_i \tag{22}$$

$$\bar{y} = \frac{1}{n}\sum_{i=1}^{n} y_i \tag{23}$$

where $\bar{x}$ and $\bar{y}$ are the mean values of x and y, respectively. The value range of Pearson's correlation coefficient is between –1 and 1. The closer value is to 1, the more significant the positive correlation between the

two variables will be. However, the closer value is to –1, the more significant the inverse correlation between the two variables will be. When the value approaches 0, it indicates that there is no linear correlation between the two variables.

Assume the null hypothesis H_0: the correlation coefficient between the two variables is not significant, then the statistic is:

$$t = r\sqrt{\frac{n-2}{1-r^2}} \tag{24}$$

where the statistic t obeys the t distribution with n–2 degrees of freedom. Given the significance level α, look up the t distribution table. If $|t|>t_{\alpha/2}$, reject the null hypothesis and consider the correlation coefficient to be significant; otherwise, it is not significant.

3 Results

3.1 Spatio-temporal variations in temperature

The spatial distribution and trends in average temperature in the ASRC from 1951 to 2019 were obtained from spline interpolation, linear trend estimation and the M-K trend test (Figs. 2 and 3). The annual and seasonal average temperature presented significant upward trends ($P < 0.01$) (Table 1). The annual average temperature was 5.83°C with an increase rate of 0.28°C/10 yr. The increase rate in seasonal temperature in descending order was winter > spring = autumn > summer. Overall, the annual and seasonal average temperature showed a gradual increase from north to southwest (Figs. 2 and 3). However, the tendency rate of seasonal average temperature varied in different regions of the ASRC, with the greatest difference in spring, followed by summer, winter, and then autumn (Fig. 3). As for annual average temperatures, 134 of 138 (97.1%) meteorological stations markedly increased at the 0.05 significance level, Tikanlik Station significantly decreased (0.7%), Alar and Mount Wutai stations increased insignificantly (1.5%), and Zedang Station did not notably decrease (0.7%) (Fig. 2). With regard to different seasons, temperatures increased significantly at 134 stations (97.1%) in spring, 126 (91.3%) in summer, 125 (90.6%) in autumn, and 123 (89.1%) in winter (Fig. 3).

3.2 Spatio-temporal variations in precipitation

According to the M-K trend test, the annual and seasonal precipitation trends were both positive, but they were only significant in spring and winter ($P < 0.05$) (Table 1). The average annual precipitation was 178.47 mm, and it increased by 3.48 mm/10 yr. The increase rate of seasonal precipitation in descending order was summer > spring > autumn > winter.

Figs. 4 and 5 show that the annual and seasonal precipitation trends were unevenly distributed. Precipitation showed a decreasing trend in the south, western central zone and northeast of the ASRC, while there was an increasing precipitation trend in the southwest, northwest, central zone and northeast of the ASRC. Of 138 stations, 30 (21.7%) had a significant increase, 3 (2.2%)

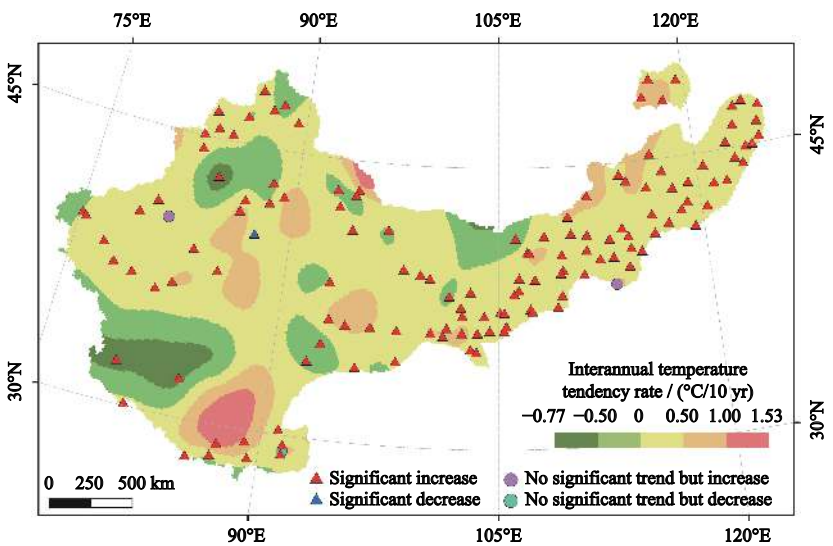

Fig. 2 Spatial characteristics of the tendency rate for annual average temperature in the arid and semiarid region of China (ASRC) from 1951 to 2019

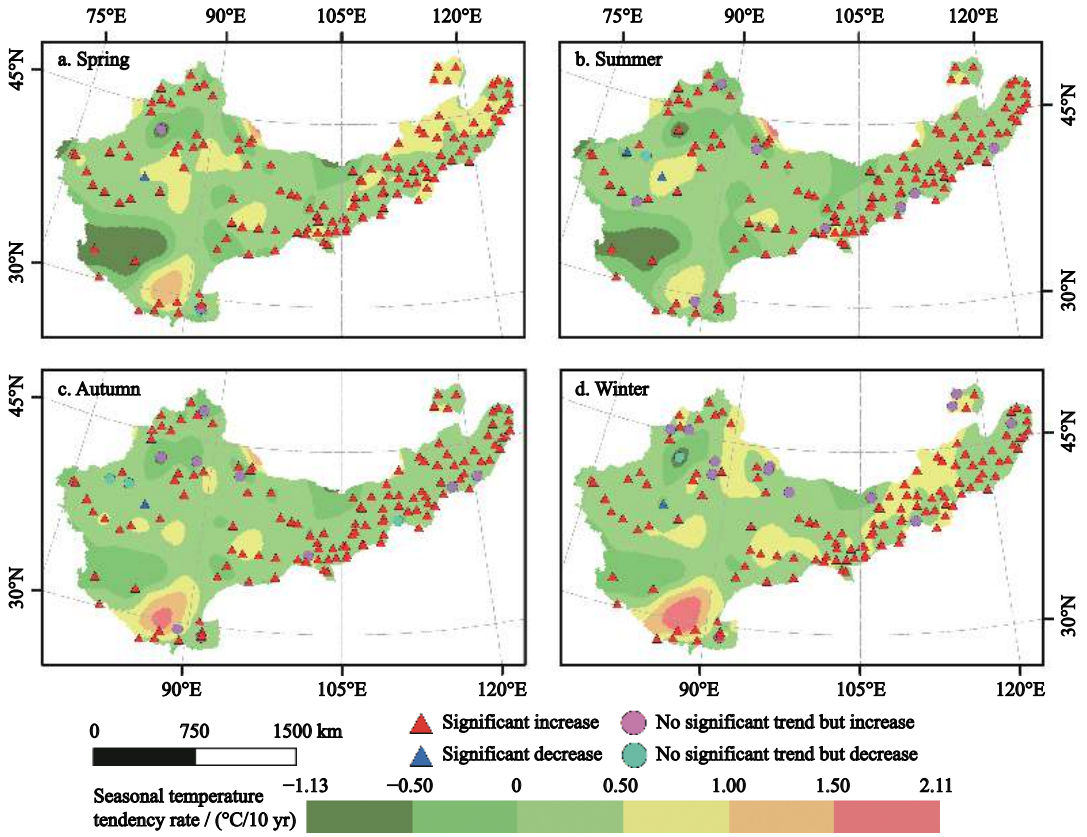

Fig. 3 Spatial distribution characteristics of the tendency rate for seasonal average temperature in the arid and semiarid region of China (ASRC) from 1951 to 2019

Table 1 Tendency rate of multi-year average temperature and precipitation in the arid and semiarid region of China (ASRC) from 1951 to 2019

Time period	Temperature		Precipitation	
	Tendency rate / (°C/10 yr)	Mean / °C	Tendency rate / (mm/10 yr)	Mean / mm
Spring	0.27**	7.61	1.00*	25.81
Summer	0.21**	19.60	1.54	117.11
Autumn	0.27**	5.78	0.76	32.22
Winter	0.35**	–9.61	0.33*	6.93
Annual	0.28**	5.83	3.48*	178.47

Note: *significant at the 0.05 level; **significant at the 0.01 level

had an obvious decrease, 60 (43.5%) had an insignificant increase, and 45 (32.6%) had an inconspicuous decreased (Fig. 4). Among the 138 stations, precipitation increased dramatically at 22.5% in spring, 14.5% in summer, 13.8% in autumn, and 18.8% in winter (Fig. 5).

3.3 Abrupt changes in temperature and precipitation

According to the M-K test, the annual average temperature increased abruptly in 2001 (Fig. 6a). Other abrupt changes in average temperature in spring, summer, autumn, and winter occurred in 2004 and 2006; 2005; 1998 and 2000; and 1989, respectively (Figs. 7a, 7b, 7c, 7d). Using the accumulative anomaly method, the abrupt change in annual average temperature was in 1997 (Fig. 6b). Abrupt temperature changes in spring, summer, autumn, and winter occurred in 1997, 1997, 1998, and 1986, respectively, which all displayed increased warming (Figs. 7e, 7f, 7g 7h). Generally, the abrupt change points in the annual and seasonal average temperature calculated by the M-K test were consistent with the results from the accumulative anomaly method,

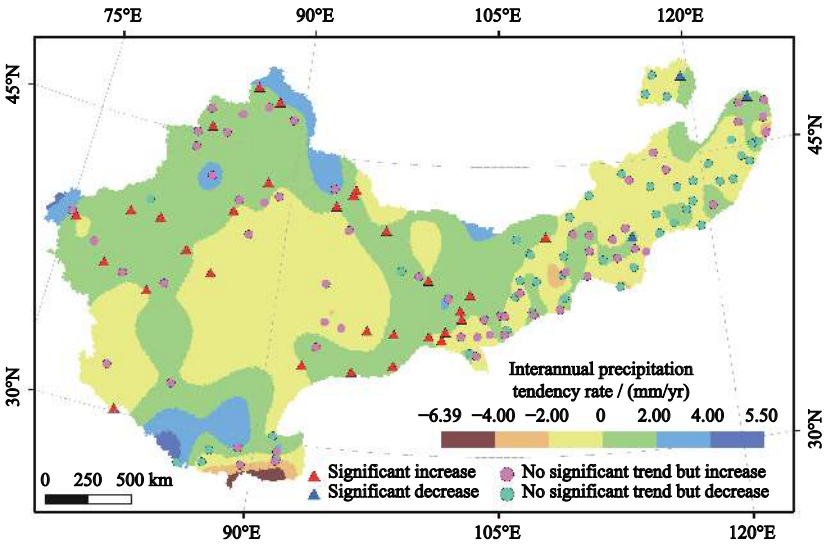

Fig. 4 Spatial distribution characteristics of the tendency rate for annual precipitation in the arid and semiarid region of China (ASRC) from 1951 to 2019

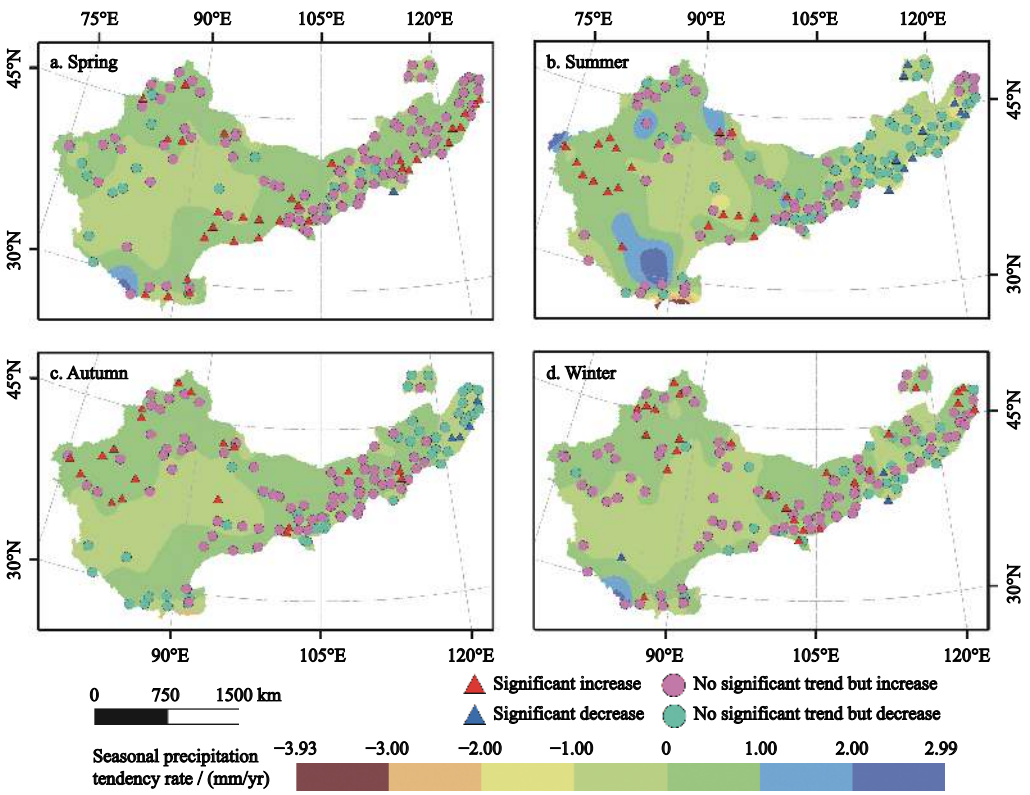

Fig. 5 Spatial distribution characteristics of the tendency rate for seasonal precipitation in the arid and semiarid region of China (ASRC) from 1951 to 2019

which indicated the abrupt changes were centered around the 1990s.

Based on the M-K test, the abrupt change years for annual precipitation were 2012, 2013, and 2014 (Fig. 8a). Abrupt changes in spring precipitation occurred in 2002, 2004, 2005, 2006, 2008, 2011 and 2012 (Fig. 9a). Changes in summer precipitation occurred in 2012, 2014, and 2016 (Fig. 9b). Abrupt changes in autumn and winter precipitation occurred only in 2008 and 2001, respectively (Figs. 9c and 9d). Using the accumulative anomaly method, the abrupt change of annual precipitation occurred in 2012 (Fig. 8b). Changes in spring,

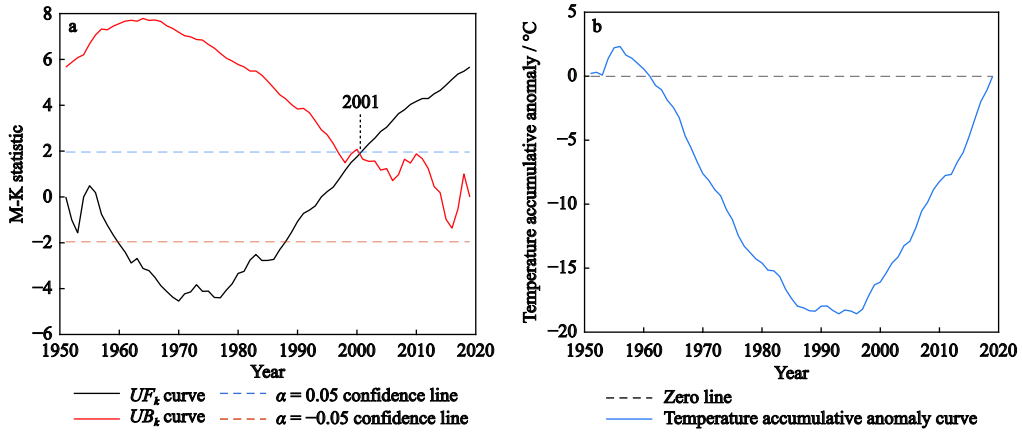

Fig. 6 M-K curve (a) and accumulative anomaly curve (b) of annual average temperature variation in the arid and semiarid region of China (ASRC) from 1951 to 2019. UF_k curve: a sequence of statistics for a positive-order time series for mutation testing; UB_k curve: a sequence of statistics for a reverse time series for mutation testing. The intersection point of the two curves is between the critical lines, that is, the corresponding time is when the mutation begins

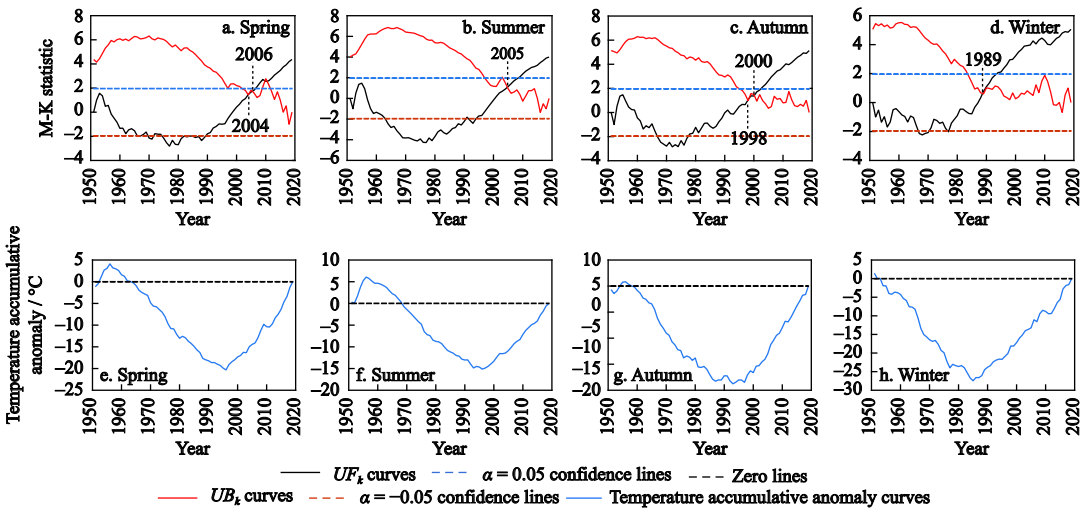

Fig. 7 M-K curves (a, b, c, and d) and accumulative anomaly curves (e, f, g, and h) of seasonal average temperature variation in the arid and semiarid region of China (ASRC) from 1951 to 2019. UF_k and UB_k curves are the same as in Fig. 6

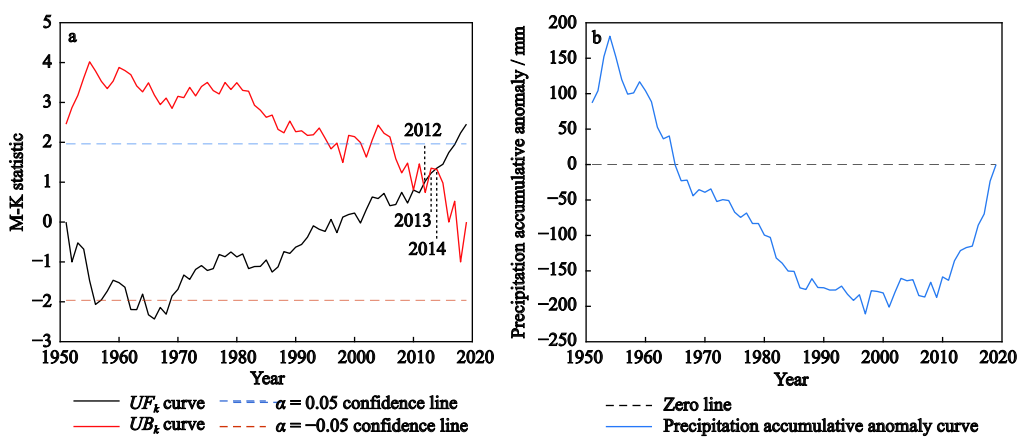

Fig. 8 M-K curve (a) and accumulative anomaly curve (b) of annual precipitation variation in the arid and semiarid region of China (ASRC) from 1951 to 2019. UF_k and UB_k curves are the same as in Fig. 6

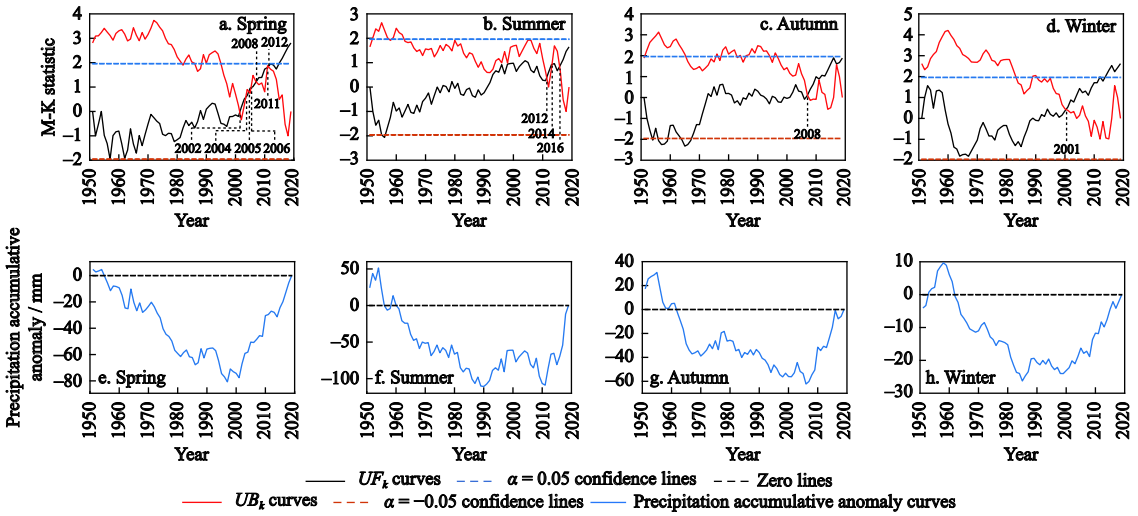

Fig. 9 M-K curves (a, b, c, and d) and accumulative anomaly curves (e, f, g, and h) of seasonal precipitation variation in the arid and semiarid region of China (ASRC) from 1951 to 2019. UF_k and UB_k curves are the same as in Fig. 6

summer, autumn, and winter precipitation occurred in 2002, 2012, 2007, and 2000, respectively (Figs. 9e, 9f, 9g, 9h). Overall, the abrupt changes time points of the annual and seasonal precipitation calculated by the two methods were similar, and mainly took place after 2000.

3.4 The correlation between atmospheric circulation, temperature and precipitation

The linear trends of the annual atmospheric circulation indices are shown in Fig. 10. The inter-decadal mean value of the AO and NAO had a similar distribution, with the maximum and minimum values in the 1990s and 1960s, respectively (Table 2). The maximum and minimum inter-decadal mean value of the PDO occurred in the 1980s and 1950s, respectively. The trends of the AO and PDO showed a marked increase, while the changes of the EASM, ENSO and NAO were not noticeable. The times of the maximum inter-decadal mean value of the AO and PDO were close to the abrupt change times in annual and seasonal average temperature.

Using the Pearson's correlation coefficient, we calculated the correlation between annual and seasonal temperature and precipitation and the atmospheric circulation indices in the ASRC (Fig. 11). The AO, EASM and PDO were significantly correlated with either the annual or a particular seasonal average temperature. The EASM had the strongest negative correlation with autumn average temperature, while the PDO had the strongest positive correlation with winter average tem-

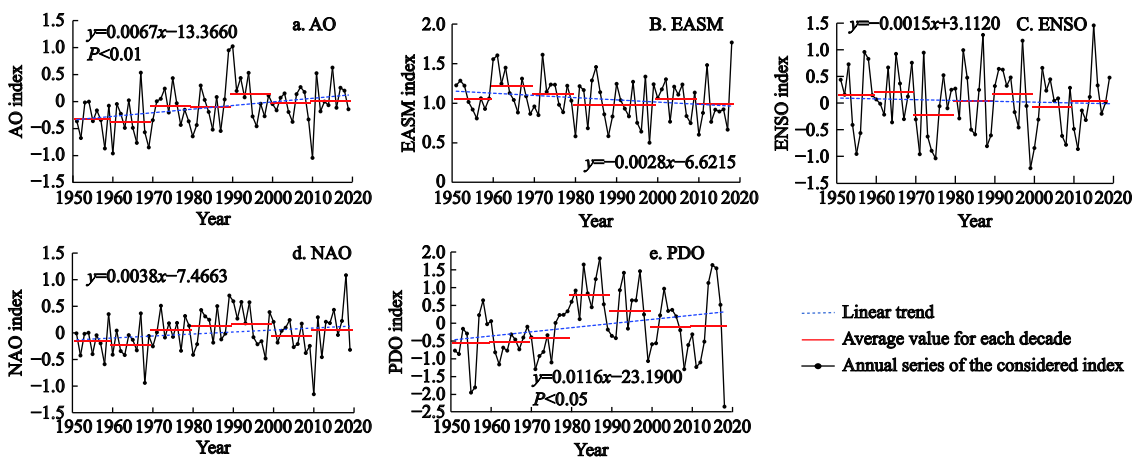

Fig. 10 Linear regression trends of annual atmospheric circulation indices from 1951 to 2019. AO: Arctic Oscillation; EASM: East Asian summer monsoon; ENSO: El Niño Southern Oscillation; NAO: North Atlantic Oscillation; PDO: Pacific Decadal Oscillation

Table 2 The occurrence time of the maximum and minimum inter-decadal mean value for the atmospheric circulation indices from 1951 to 2019

Atmospheric circulation indices	The time of the maximum inter-decadal mean	The time of the minimum inter-decadal mean
AO	1990s	1960s
EASM	1960s	1990s
ENSO	1960s	1970s
NAO	1990s	1960s
PDO	1980s	1950s

Notes: AO, Arctic Oscillation; EASM, East Asian summer monsoon; ENSO, El Niño Southern Oscillation; NAO, North Atlantic Oscillation; PDO, Pacific Decadal Oscillation.

perature. In contrast, there were no clear correlations between ENSO and NAO and annual and seasonal average temperature. It should be noted that the correlations between all atmospheric circulation indices and precipitation were insignificant.

Figs. 12 and 13 illustrate the Pearson's correlation coefficients between the atmospheric circulation indices and annual and seasonal average temperature as well as precipitation in the abrupt change years. In the abrupt change years, there were significant correlations between annual average temperature or precipitation and at least one atmospheric circulation index. The EASM had the strongest positive correlation with the annual average temperature in 2006 and annual precipitation in 2008. The NAO had the strongest negative correlation with the temperature and precipitation in 1998 and 2016, respectively. There was also a high correlation between ENSO and average temperature and pre-

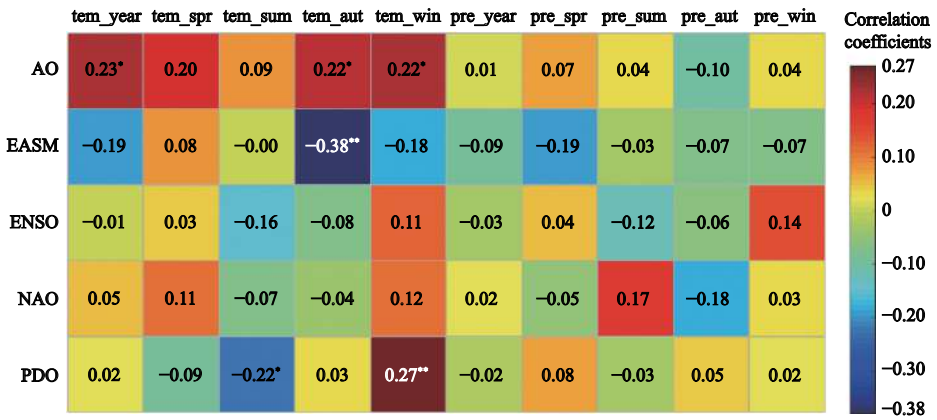

Fig. 11 Correlation between atmospheric circulation indices and annual and seasonal average temperature and precipitation in the arid and semiarid region of China (ASRC) during 1951–2019. *significant at the 0.1 level; **significant at the 0.05 level; tem_year: annual average temperature; tem_spr: spring average temperature; tem_sum: summer average temperature; tem_aut: autumn average temperature; tem_win: winter average temperature; pre_year: annual precipitation; pre_spr: spring precipitation; pre_sum: summer precipitation; pre_aut: autumn precipitation; pre_win: winter precipitation; AO, EASM, ENSO, NAO and PDO are the same as Fig. 10

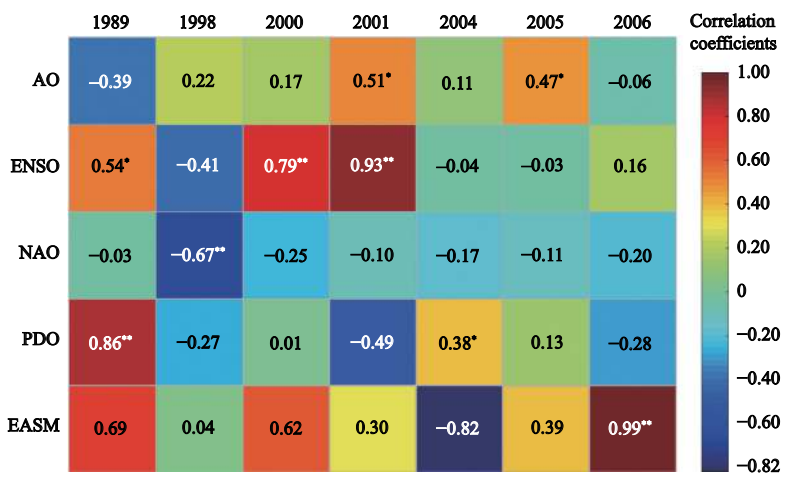

Fig. 12 Pearson's correlation coefficients between atmospheric circulation indices and annual average temperature in abrupt change years in the arid and semiarid region of China (ASRC) during 1951–2019. *significant at the 0.1 level; **significant at the 0.05 level. AO, EASM, ENSO, NAO and PDO are the same as Fig. 10

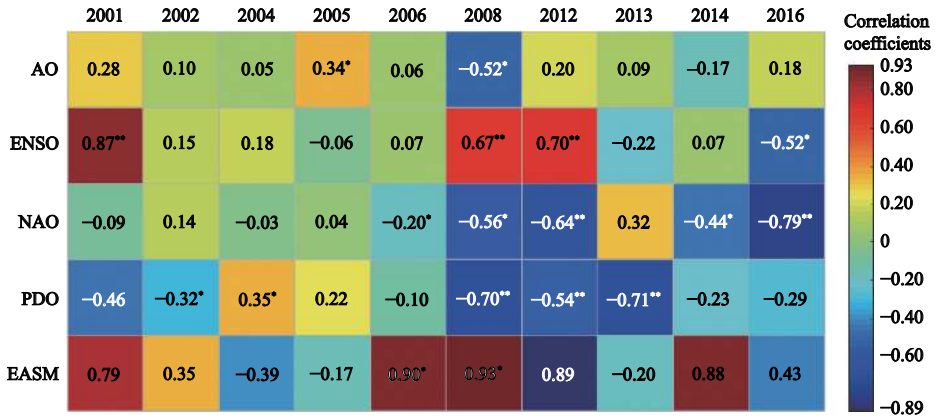

Fig. 13 Pearson's correlation coefficients between atmospheric circulation indices and annual precipitation in abrupt change years in the arid and semiarid region of China (ASRC) during 1951–2019. *significant at the 0.1 level; **significant at the 0.05 level. AO, EASM, ENSO, NAO and PDO are the same as Fig. 10

cipitation in the abrupt change years. The annual precipitation in 2008 was significantly correlated with each atmospheric circulation index.

4 Discussion

4.1 Effects of anthropogenic and natural factors on temperature and precipitation

Population increases and economic development have accelerated the use of fossil fuels and carbon dioxide emissions since the 1950s in China; these directly contribute to the greenhouse effect and affect the surface temperature (Karl and Trenberth, 2003; Jiang, 2010; Zhang, 2019). The ASRC is no exception. According to the analysis of the total population and energy consumption of the 12 provinces involved by the ASRC, both the population and energy consumption were on the rise after 1950 and 1985, respectively (Fig. 14). Their correlation coefficient was 0.89 at the level of significance of 0.05, indicating that they had a very high positive correlation. A plenty of nitrogen oxides produced by socio-economic activities and excessive use of chlorofluorocarbons have resulted in worsening air pollution, which damages the ozone layer, warms the lower atmosphere, cools the upper atmosphere, and aggravates climate warming (Kuang, 2000; Luo et al., 2019). Human activities have also expedited methane production. As referenced by Ji et al. (2014), winter heating increases the consumption of natural gas composed mainly of methane, which directly produces more greenhouse gases and lead to more marked warming in winter. This is consistent with our research.

Dramatic land cover changes of the underlying surface have exacerbated drought, land salinization and desertification, resulting in an increase in surface radiation and a reduction in ecological resilience; this is one of the causes of temperature rise in the ASRC (Guan and Hao, 2013; Li et al., 2015). Social development and migration to cities has also accelerated urbanization. The conversion of green spaces to impervious surfaces has led to an 'urban heat island effect' whereby the urban temperature is significantly higher than that of surrounding areas (Xue et al., 2019; Yan et al., 2020). In addition, the destruction of natural landscapes during

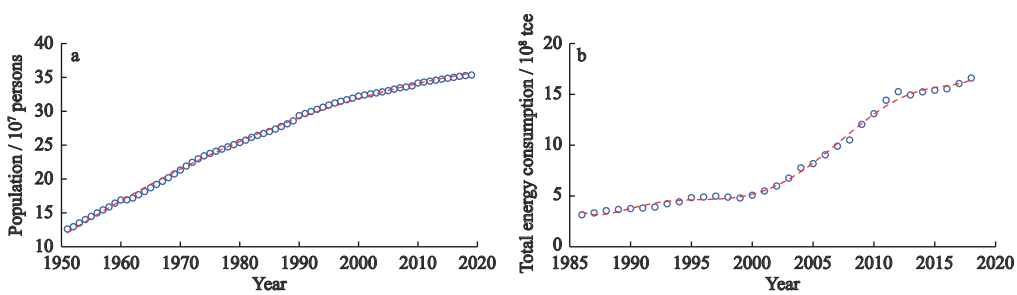

Fig. 14 Changes of total population (a) and energy consumption (b) in the arid and semiarid region of China (ASRC). tce: tons of coal equivalent

development greatly reduces their ability to absorb carbon dioxide, leading to warming temperatures (John, 2009). However, owing to the implementation of forest conservation and tree planting schemes, such as the 'Three-North Forest Protection Project' and 'Returning Farmland to Forest and Grassland' policy, China's land cover has become noticeably greener (Chen et al., 2019). As referenced by Yu et al. (2020), the vegetation coverage on the Loess Plateau increased significantly from 2001 to 2017, which led to an increase in precipitation in this region. Sand-fixing and afforestation in the Kubuqi Desert and Mu Us Desert has proved effective in desert greening (Zheng et al., 2020). One study has reported that, owing to the implementation of ecological engineering, the desert areas of the Tarim and Qaidam basins have seen rainfall for three consecutive years (Li et al., 2021c). Overall, the areas that have carried out ecological projects are consistent with those with increased precipitation and cooler temperatures in our study area.

Due to the periodic changes in the Earth's orbit, regular oscillations in the temperature between high and low has exerted influences on precipitation (Mao et al, 2016; Ahluwalia, 2019). This explains why there is more precipitation in summer and less precipitation in winter in our survey region. Correspondingly, solar activities affect the temperature. The research of Huang et al. (2020) shows that the intensity of solar activities has increased significantly in the past 100 years, which is consistent with the global temperature rise over the same period. In addition, atmospheric circulation also plays a critical role in regional temperature and precipitation through teleconnection (Yang et al., 2020; Zhang et al., 2021). The AO and ENSO have significant correlations with temperature changes in northern China (Gong et al., 2009; Tong et al., 2019). Our study found strong correlations between atmospheric circulation indices and trends and abrupt changes in average temperature as well as in precipitation.

To sum up, the spatio-temporal variations of temperature and precipitation in the ASRC are influenced by long-term and short-term as well as by direct and indirect anthropogenic and natural factors. Human activities play a dominant role through two contrasting pathways. On the one hand, the degradation of natural ecosystem caused by anthropogenic activities has largely increased climate warming and abrupt change. On the other hand, the implementation of ecological conservation engineering has mitigated or diminished the negative influence on climate change.

4.2 Potential influences of temperature and precipitation changes on the ASRC

From 1951 to 2019, the annual average temperature and annual precipitation increased by about 1.93°C and 24 mm in the ASRC, respectively. Lyu et al. (2009) found that the temperature of the ASRC rose by about 1.8°C and precipitation increased by about 29 mm in the early 21st century compared with that in the 1960s, which is similar to our results. The rise in temperature would prolong the growing season, facilitate the growth of thermophilic crops, and expand the suitable planting area (Gao et al., 2011; Lu et al., 2021). In the context of a warming climate, summer monsoons possess greater quantities of warm and moist air but also have a more widespread effect in inland areas, which brings more precipitation to the ASRC (Chen et al., 2007; Famiglietti, 2014). Adequate precipitation brings suitable conditions for the growth of crops and plants, which is beneficial for increasing grain yields and grassland areas (Zheng et al., 2021). In addition, more precipitation increases surface moisture and facilitates the agglomeration of soil particles, which further promotes vegetation growth and decreases the risk of natural disasters as well as reducing water and soil erosion in the region (Gong et al., 2020).

The underlying negative effects should also be given sufficient attentions. If there is only a small rise in precipitation, the water levels of inland rivers and lakes will decline because a warmer climate will increase evaporation (Li et al., 2011; Fuentes et al., 2021). In addition, the frequency of drought and flood disasters will increase because of greater variability of water resources (Abbasian et al., 2021). Meanwhile, domestic and industrial water use would be limited by growing supply–demand conflicts over water resources (Zhang et al., 2015). Moreover, a warming climate will exacerbate pests and diseases, reduce grain yields and degrade grasslands (Macfadyen et al., 2018; Lee et al., 2021). It also should be noted that, in areas with higher temperatures and less precipitation, the likelihood of sand or dust formation will be accelerated, giving rise to intensified sandstorm activity (Vicente-Serrano et al., 2020). In addition, the urban heat island effect caused by high temperature will harm human health and perturb ecosystem stability (Santamouris, 2020).

4.3 Suggestions for climate change responses and environmental protection

Regional comparative studies of climate change are an effective way to understand the driving forces of eco-environmental impacts in different areas. According to our research results, the following suggestions are proposed to respond to climate change and protect the eco-environment.

First, measures for energy conservation and emission reduction should be enforced and strengthen in all aspects of the society to enhance the sustainability of urban development. More effective approaches and techniques should also be developed to mitigate or curb greenhouse gas emissions at source.

Second, adequate attention should be given to urban planning for sustainable development goals so that the use of land resources is more reasonable and the negative effects of human activities on natural ecosystems are minimized. Stricter planning controls should also be established to avoid the arbitrary conversion of vegetation to impervious surfaces to alleviate the urban heat island effect.

Third, ecological projects should continue to be carried out to mitigate the adverse effects of climate change and enhance the ability of ecosystems to withstand natural disasters. The establishment of a monitoring system can provide effective feedback on all aspects of ecological engineering and provide a reference for subsequent research and the formulation of strategies.

Finally, climate change is a borderless issue; thus, multilateral cooperation mechanisms should be established with neighboring countries to respond to regional or global climate change. Only when governments and people across the world pay attention to climate change will climate problems be effectively addressed at regional and global scales.

4.4 Advantages and limitations of the study

The analysis of climate change characteristics in our research was carried out using a synthesized rather than an isolated perspective. The spatio-temporal patterns of both temperature and precipitation in the ASRC were comprehensively analyzed and their variations were accurately reflected. Most previous research on meteorological factors has focused on analyzing climate trends and abrupt changes. Few studies have examined the driving factors affecting climate change. In our study, the correlation between several atmospheric circulation indices and temperature and precipitation was explored and their impacts on climate were determined. This provided a novel way to analyze the causes of climate change. In addition, the identification of abrupt changes in temperature and precipitation in previous studies often used only one test, which hindered validation of the results. Here, two change analysis methods, i.e., the M-K test and accumulative anomaly method, were used to determine abrupt changes in temperature and precipitation, which improved the reliability of our results. Furthermore, our study focused on the ASRC, which contains ecosystems that are vulnerable to climate change. This region has been little-studied and our results help to address the research deficiency in regional climate change.

There are also some uncertainties and limitations in our study. Since climate change is a long-term and complex process, it is important to explore the variation in climate factors with a longer time series (Bova et al., 2021). Our study looked at temperature and precipitation over only 69 years, a short period relative to the Earth's macro-cyclical climate stages; this increases the uncertainty of our findings. Therefore, research on the longer-term reconstruction and prediction of meteorological change needs to be carried out for more precise determination of climate change in the future. Furthermore, there are multitudinous factors that impact the climate change owing to the interactions between the internal climate system and external factors. In addition to the influencing factors discussed in this study, there are still other factors that contribute to climate change. However, due to the difficulty of data acquisition, other factors were not analyzed. It is necessary to conduct more extensive and in-depth studies on the influencing factors of climate change in the future so as to provide more reliable reference to deal with climate issues.

5 Conclusions

Research on the characteristics and changes in the climate is crucial to develop a climate change response and for eco-environmental protection, and helps to formulate government policies. We combined a trend test, abrupt change test and correlation analysis to discern variations in annual and seasonal average temperature and precipitation as well as their influencing factors in the

ASRC from 1951 to 2019. The results showed that both the annual average temperature and annual precipitation increased: temperature rose at a rate of 0.28°C/10 yr and precipitation at a rate of 3.48 mm/10 yr. The trends for seasonal average temperatures significantly increased, with abrupt changes mainly occurring around the 1990s. The trend for seasonal precipitation showed significant increases in spring and winter, principally after 2000. The spatio-temporal variations of temperature and precipitation differed across the region, with the southwest ARSC showing the most obvious variation in each season. Atmospheric circulation, especially the EASM, had a major effect on trends and abrupt changes in temperature and precipitation. Human activities are the dominant factors driving variations in temperature and precipitation. Our findings can be used as a reference for multilateral government policies to effectively respond to climate change.

References

Abbasian M S, Najafi M R, Abrishamchi A, 2021. Increasing risk of meteorological drought in the Lake Urmia basin under climate change: introducing the precipitation-temperature deciles index. *Journal of Hydrology*, 592: 125586. doi: 10.1016/J.JHYDROL.2020.125586

Ahluwalia H S, 2019. Changes of space weather and space climate at Earth orbit: an update. *Advances in Space Research*, 64(5): 1093–1099. doi: 10.1016/j.asr.2019.05.046

Bova S, Rosenthal Y, Liu Z Y et al., 2021. Seasonal origin of the thermal maxima at the Holocene and the last interglacial. *Nature*, 589(7843): 548–553. doi: 10.1038/s41586-020-03155-x

Carrasco J F, Cordero R R, 2020. Analyzing precipitation changes in the northern tip of the Antarctic peninsula during the 1970–2019 period. *Atmosphere*, 11(12): 1270. doi: 10.3390/ATMOS11121270

Chen C, Park T, Wang X H et al., 2019. China and India lead in greening of the world through land-use management. *Nature Sustainability*, 2(2): 122–129. doi: 10.1038/s41893-019-0220-7

Chen F L, Chen H M, Yan Y Y, 2015. Annual and seasonal changes in means and extreme events of precipitation and their connection to elevation over Yunnan Province, China. *Quaternary International*, 374: 46–61. doi: 10.1016/j.quaint.2015.02.016

Chen Y N, Li W H, Xu C C et al., 2007. Effects of climate change on water resources in Tarim River Basin, Northwest China. *Journal of Environmental Sciences*, 19(4): 488–493. doi: 10.1016/S1001-0742(07)60082-5

Dai A G, Fung I Y, Del Genio A D, 1997. Surface observed global land precipitation variations during 1900–88. *Journal of Climate*, 10(11): 2943–2962. doi: 10.1175/1520-0442(1997)010<2943:SOGLPV>2.0.CO;2

Famiglietti J S, 2014. The global groundwater crisis. *Nature Climate Change*, 4(11): 945–948. doi: 10.1038/nclimate2425

Feng Q, Li Z X, Liu W et al., 2016. Relationship between large scale atmospheric circulation, temperature and precipitation in the Extensive Hexi region, China, 1960–2011. *Quaternary International*, 392: 187–196. doi: 10.1016/j.quaint.2015.06.015

Fuentes I, Fuster R, Avilés D et al., 2021. Water scarcity in central Chile: the effect of climate and land cover changes on hydrologic resources. *Hydrological Sciences Journal*, 66(6): 1028–1044. doi: 10.1080/02626667.2021.1903475

Gao Tao, Chen Yancai, Yu Xiao, 2011. Analysis on effects of global warming on three major crop yields in Inner Mongolia. *Chinese Journal of Agrometeorology*, 32(03): 407–416. (in Chinese)

Ge Q S, Zhang X Z, Hao Z X et al., 2011. Rates of temperature change in China during the past 2000 years. *Science China Earth Sciences*, 54(11): 1627–1634. doi: 10.1007/s11430-011-4257-3

Gocic M, Trajkovic S, 2013. Analysis of changes in meteorological variables using Mann-Kendall and Sen's slope estimator statistical tests in Serbia. *Global and Planetary Change*, 100: 172–182. doi: 10.1016/j.gloplacha.2012.10.014

Gong Y H, Zhao D M, Ke W B et al., 2020. Legacy effects of precipitation amount and frequency on the aboveground plant biomass of a semi-arid grassland. *Science of the Total Environment*, 705: 135899. doi: 10.1016/j.scitotenv.2019.135899

Gong Zhiqiang, Wang Xiaojuan, Zhi Rong et al., 2009. Regional characteristics of temperature changes in China during the past 58 years and its probable correlation with abrupt temperature change. *Acta Physica Sinica*, 58(6): 4342–4353. (in Chinese). doi: 10.7498/aps.58.4342

Gou J J, Miao C Y, Han J Y, 2020. Spatiotemporal changes in temperature and precipitation over the Songhua River Basin between 1961 and 2014. *Global Ecology and Conservation*, 24: e01261. doi: 10.1016/J.GECCO.2020.E01261

Guan Zhongmei, Hao Chengyuan, 2013. The fragile ecosystem types in arid and semi-arid region of China and their degradation causes. *Ecological Economy*, (9): 158–162. (in Chinese)

Hansen J, Ruedy R, Sato M et al., 2001. A closer look at United States and global surface temperature change. *Journal of Geophysical Research*, 106(D20): 23947–23963. doi: 10.1029/2001JD000354

Huang C, Rao Z G, Li Y X et al., 2020. Holocene summer temperature in arid central Asia linked to millennial-scale North Atlantic climate events and driven by centennial-scale solar activity. *Palaeogeography, Palaeoclimatology, Palaeoecology*, 556: 109880. doi: 10.1016/j.palaeo.2020.109880

Huang J P, Ma J R, Guan X D at al., 2019. Progress in Semi-arid Climate Change Studies in China. *Advances in Atmospheric Sciences*, 36(9): 922–937. doi: 10.1007/s00376-018-8200-9

Ji F, Wu Z H, Huang J P et al., 2014. Evolution of land surface air temperature trend. *Nature Climate Change*, 4(6): 462–466. doi: 10.1038/nclimate2223

Jia Yang, Cui Peng, 2018. Contrastive analysis of temperature interpolation at different time scales in the alpine region by Anusplin. *Plateau Meteorology*, 37(3): 757–766. (in Chinese)

Jiang Z, 2010. Reflections on energy issues in China. *In:Jiang Z M (ed). Research on Energy Issues in China. Amsterdam:Aca-*

demic Press, 257–274. doi: 10.1016/B978-0-12-378619-7.00002-6

Jobst A M, Kingston D G, Cullen N J et al., 2017. Combining thin-plate spline interpolation with a lapse rate model to produce daily air temperature estimates in a data-sparse alpine catchment. *International Journal of Climatology*, 37(1): 214–229. doi: 10.1002/joc.4699

John R, Chen J Q, Lu N et al., 2009. Land cover/land use change in semi-arid Inner Mongolia: 1992–2004. *Environmental Research Letters*, 4(4): 045010. doi: 10.1088/1748-9326/4/4/045010

Karl T R, Trenberth K E, 2003. Modern global climate change. *Science*, 302(5651): 1719–1723. doi: 10.1126/science.1090228

Kerr R A, 2007. Global warming is changing the world. *Science*, 316(5822): 188–190. doi: 10.1126/science.316.5822.188

Kuang Yuehui, 2000. On the hot spot at the turning-point of the century: environmental pollution. *China Population, Resources and Environment*, 10(S1): 44–46. (in Chinese)

Lee R H, Navarro-Navarro L A, Ley A L et al., 2021. Spatio-temporal dynamics of climate change, land degradation, and water insecurity in an arid rangeland: the Río San Miguel watershed, Sonora, Mexico. *Journal of Arid Environments*, 193: 104539. doi: 10.1016/J.JARIDENV.2021.104539

Li Hongyu, Fu Congbin, Guo Weidong et al., 2015. Study of energy partitioning and its feedback on the microclimate over different surfaces in an arid zone. *Acta Physica Sinica*, 64(5): 059201. (in Chinese). doi: 10.7498/aps.64.059201

Li J, Wang J L, Zhang J et al., 2021a. Dynamic changes of vegetation coverage in China-Myanmar economic corridor over the past 20 years. *International Journal of Applied Earth Observation and Geoinformation*, 102: 102378. doi: 10.1016/J.JAG.2021.102378

Li Junli, Chen Xi, Bao Anming, 2011. Spatial-temporal characteristics of lake level changes in central Asia during 2003–2009. *Acta Geographica Sinica*, 66(9): 1219–1229. (in Chinese)

Li M X, Ping F, Tang X B et al., 2019. Effects of microphysical processes on the rapid intensification of Super-Typhoon Meranti. *Atmospheric Research*, 219: 77–94. doi: 10.1016/j.atmosres.2018.12.031

Li Q X, Sun W B, Yun X et al. , 2021b. An updated evaluation of the global mean land surface air temperature and surface temperature trends based on CLSAT and CMST. Climate Dynamics, 56(1–2): 635–650. doi: 10.1007/S00382-020-05502-0

Li T X, Zhou Z Q, Fu Q et al., 2020a. Analysis of precipitation changes and its possible reasons in Songhua River Basin of China. *Journal of Water and Climate Change*, 11(3): 839–864. doi: 10.2166/wcc.2019.250

Li W J, Liu J P, Chen L J et al., 2014. Spatiotemporal distribution and decadal change of the monthly temperature predictability limit in China. *Chinese Science Bulletin*, 59(34): 4864–4872. doi: 10.1007/s11434-014-0502-4

Li W W, Huang F, Shi F Z et al., 2021c. Human and climatic drivers of land and water use from 1997 to 2019 in Tarim River basin, China. *International Soil and Water Conservation Research*, 9(4): 532–543. doi: 10.1016/J.ISWCR.2021.05.001

Li Y, Qin Y C, Ma L Q et al., 2020b. Climate change: vegetation and phenological phase dynamics. *International Journal of Climate Change Strategies and Management*, 12(4): 495–509. doi: 10.1108/IJCCSM-06-2019-0037

Lu H L, Jing W L, Zhao J C et al., 2014. Characteristics of the temporal variation in temperature and precipitation in China's lower Yellow River region. *Advances in Meteorology*, 2014: 186823. doi: 10.1155/2014/186823

Lu M G, Sun H W, Yan D et al., 2021. Projections of thermal growing season indices over China under global warming of 1.5°C and 2. 0°C. *Science of the Total Environment*, 781: 146774. doi: 10.1016/J.SCITOTENV.2021.146774

Lyu Yan, Wang Ranghui, Cai Ziying, 2009. Climatic change and influence in arid and semi-arid area of China. *Journal of Arid Land Resources and Environment*, 23(11): 65–71. (in Chinese)

Luo Z B, Lam S K, Fu H et al., 2019. Temporal and spatial evolution of nitrous oxide emissions in China: assessment, strategy and recommendation. *Journal of Cleaner Production*, 223: 360–367. doi: 10.1016/j.jclepro.2019.03.134

Macfadyen S, McDonald G, Hill M P, 2018. From species distributions to climate change adaptation: knowledge gaps in managing invertebrate pests in broad-acre grain crops. *Agriculture, Ecosystems & Environment*, 253: 208–219. doi: 10.1016/j.agee.2016.08.029

Mao D H, Luo L, Wang Z M et al., 2018a. Conversions between natural wetlands and farmland in China: a multiscale geospatial analysis. *Science of the Total Environment*, 634: 550–560. doi: 10.1016/j.scitotenv.2018.04.009

Mao D H, Wang Z M, Wu B F et al., 2018b. Land degradation and restoration in the arid and semiarid zones of China: quantified evidence and implications from satellites. *Land Degradation & Development*, 29(11): 3841–3851. doi: 10.1002/ldr.3135

Mao Kebiao, Zuo Zhiyuan, Zhu Gaofeng et al. , 2016. Study of the relationship between global climate-ecosystem 's change and planetary orbit position 's change. Chinese High Technology Letters, 26(10–11): 890–899. (in Chinese)

McGregor A, 2010. Sovereignty and the responsibility to protect: the case of Cyclone Nargis. *Political Geography*, 29(1): 3–4. doi: 10.1016/j.polgeo.2009.09.002

Ni J, 2011. Impacts of climate change on Chinese ecosystems: key vulnerable regions and potential thresholds. *Regional Environmental Change*, 11(1): 49–64. doi: 10.1007/s10113-010-0170-0

Peterson T C, Vose R S, 1997. An overview of the global historical climatology network temperature database. *Bulletin of the American Meteorological Society*, 78(12): 2837–2850. doi: 10.1175/1520-0477(1997)078<2837:AOOTGH>2.0.CO;2

Press F, 2008. Earth science and society. *Nature*, 451(7176): 301–303. doi: 10.1038/nature06595

Raker E J, Lowe S R, Arcaya M C et al., 2019. Twelve years later: the long-term mental health consequences of Hurricane Katrina. *Social Science & Medicine*, 242: 112610. doi: 10.1016/j.socscimed.2019.112610

Santamouris M, 2020. Recent progress on urban overheating and heat island research. *Integrated assessment of the energy, environmental, vulnerability and health impact. Synergies with the global climate change. Energy and Buildings*, 207: 109482. doi: 10.1016/j.enbuild.2019.109482

Schweinsberg S, Darcy S, Beirman D, 2020. 'Climate crisis' and

'bushfire disaster': implications for tourism from the involvement of social media in the 2019–2020 Australian bushfires. *Journal of Hospitality and Tourism Management*, 43: 294–297. doi: 10.1016/j.jhtm.2020.03.006

Sensuse D I, Cahyaningsih E, Wibowo W C, 2015. Identifying knowledge management process of Indonesian government human capital management using analytical hierarchy process and Pearson correlation analysis. *Procedia Computer Science*, 72: 233–243. doi: 10.1016/j.procs.2015.12.136

Shi J, Cui L L, Wang J B et al., 2019. Changes in the temperature and precipitation extremes in China during 1961–2015. *Quaternary International*, 527: 64–78. doi: 10.1016/j.quaint.2018.08.008

Song B, Park K, 2020. Temperature trend analysis associated with land-cover changes using time-series data (1980–2019) from 38 weather stations in South Korea. *Sustainable Cities and Society*, 65: 102615. doi: 10.1016/J.SCS.2020.102615

Song X Y, Song S B, Sun W Y et al., 2015. Recent changes in extreme precipitation and drought over the Songhua River Basin, China, during 1960–2013. *Atmospheric Research*, 157: 137–152. doi: 10.1016/j.atmosres.2015.01.022

Tong S Q, Li X Q, Zhang J Q et al., 2019. Spatial and temporal variability in extreme temperature and precipitation events in Inner Mongolia (China) during 1960–2017. *Science of the Total Environment*, 649: 75–89. doi: 10.1016/J.SCITOTENV.2018.08.262

Vicente-Serrano S M, Quiring S M, Peña-Gallardo M et al. , 2020. A review of environmental droughts: increased risk under global warming? Earth-Science Reviews, 201: 102953. doi: 10.1016/j.earscirev.2019.102953

Wang R, Zhang J Q, Guo E L et al., 2019. Spatial and temporal variations of precipitation concentration and their relationships with large-scale atmospheric circulations across Northeast China. *Atmospheric Research*, 222: 62–73. doi: 10.1016/j.atmosres.2019.02.008

Wang T, Wang H J, Otterå O H et al., 2013. Anthropogenic agent implicated as a prime driver of shift in precipitation in eastern China in the late 1970s. *Atmospheric Chemistry and Physics*, 13(24): 12433–12450. doi: 10.5194/acp-13-12433-2013

Wen X H, Wu X Q, Gao M, 2017. Spatiotemporal variability of temperature and precipitation in Gansu Province (Northwest China) during 1951–2015. *Atmospheric Research*, 197: 132–149. doi: 10.1016/j.atmosres.2017.07.001

Xu Xiang, Xu Yao, Sun Qingqing et al., 2018. Comparision study on meteorological spatial interpolation approaches in Kangdian region of China. *Journal of Huazhong Normal University (Natural Sciences)*, 52(1): 122–129. (in Chinese)

Xu Y Y, Sun H, Ji X, 2021. Spatial-temporal evolution and driving forces of rainfall erosivity in a climatic transitional zone: a case in Huaihe River Basin, eastern China. *CATENA*, 198: 104993. doi: 10.1016/J.CATENA.2020.104993

Xue J, Gui D W, Lei J Q et al., 2019. Oasification: an unable evasive process in fighting against desertification for the sustainable development of arid and semiarid regions of China. *CATENA*, 179: 197–209. doi: 10.1016/j.catena.2019.03.029

Yan B, Lu Z H, Yao L Q et al., 2021. Analysis on the characteristics of precipitation changes in the Yangtze River Basin in recent years. *IOP Conference Series:Earth and Environmental Science*, 768(1): 012050. doi: 10.1088/1755-1315/768/1/012050

Yan Zhongwei, Ding Yihui, Zhai Panmao et al., 2020. Re-assessing climatic warming in China since the last century. *Acta Meteorologica Sinica*, 78(3): 370–378. (in Chinese)

Yang Y, Gao M, Xie N R et al., 2020. Relating anomalous large-scale atmospheric circulation patterns to temperature and precipitation anomalies in the East Asian monsoon region. *Atmospheric Research*, 232: 104679. doi: 10.1016/j.atmosres.2019.104679

Yu L X, Liu Y, Liu T X et al., 2020. Impact of recent vegetation greening on temperature and precipitation over China. *Agricultural and Forest Meteorology*, 295: 108197. doi: 10.1016/j.agrformet.2020.108197

Zhang L, Liu Y F, Zhan H B et al., 2021. Influence of solar activity and EI Niño-Southern Oscillation on precipitation extremes, streamflow variability and flooding events in an arid-semiarid region of China. *Journal of Hydrology*, 601: 126630. doi: 10.1016/J.JHYDROL.2021.126630

Zhang L J, Li Y S, Zhang F et al., 2020. Changes of winter extreme precipitation in Heilongjiang province and the diagnostic analysis of its circulation features. *Atmospheric Research*, 245: 105094. doi: 10.1016/j.atmosres.2020.105094

Zhang Q, Singh V P, Li J F et al., 2011. Analysis of the periods of maximum consecutive wet days in China. *Journal of Geophysical Research*, 116(D23): D23106. doi: 10.1029/2011JD016088

Zhang Qiang, Yao Yubi, Li Yaohui et al., 2015. Research progress and prospect on the monitoring and early warning and mitigation technology of meteorological drought disaster in Northwest China. *Advances in Earth Science*, 30(2): 196–213. (in Chinese)

Zhang Yi, 2019. China's population transition over the past 70 years since the founding of the People's Republic of China and future policy reform. *Studies on Socialism with Chinese Characteristics*, (4): 18–30. (in Chinese)

Zhao Y M, Luo Y, 2021. Wavelet analysis on temperature and precipitation changes in Dabie Mountain of West Anhui. *Journal of Physics:Conference Series*, 1732: 012105. doi: 10.1088/1742-6596/1732/1/012105

Zhao Zhen, 2019. Multi-satellite observations on the structure characteristics of typhoon Meranti in 2016. *Plateau Meteorology*, 38(1): 156–164. (in Chinese)

Zheng K Y, Tan L S, Sun Y W et al., 2021. Impacts of climate change and anthropogenic activities on vegetation change: evidence from typical areas in China. *Ecological Indicators*, 126: 107648. doi: 10.1016/j.ecolind.2021.107648

Zheng Y, Dong L, Xia Q et al., 2020. Effects of revegetation on climate in the Mu Us Sandy Land of China. *Science of the Total Environment*, 739: 139958. doi: 10.1016/j.scitotenv.2020.139958

Zhong Y W, Li J B, 2014. Runoff variation trend of three diversions in recent 60 years and the analysis of influencing factors. Advanced Materials Research, 955–959: 3032–3035. doi: 10.4028/www.scientific.net/AMR.955-959.3032